Homogeneous Catalysis

Cationic Zinc Hydride Catalyzed Carbon Dioxide Reduction to Formate: Deciphering Elementary Reactions, Isolation of Intermediates, and Computational Investigations

Raju Chambenahalli,[a] R. M. Bhargav,[a] Karl N. McCabe,[b] Alex P. Andrews,[a] Florian Ritter,[c] Jun Okuda,[c] Laurent Maron,*[b] and Ajay Venugopal*[a]

Abstract: Zinc has been an element of choice for carbon dioxide reduction in recent years. Zinc compounds have been showcased as catalysts for carbon dioxide hydrosilylation and hydroboration. The extent of carbon dioxide reduction can depend on various factors, including electrophilicity at the zinc center and the denticity of the ancillary ligands. In a few cases, the addition of Lewis acids to zinc hydride catalysts markedly influences carbon dioxide reduction. These factors have been investigated by exploring elementary reactions of carbon dioxide hydrosilylation and hydroboration by using cationic zinc hydrides bearing tetradentate tris[2-(dimethylamino)ethyl]amine and tridentate *N*,*N*,*N*′,*N*′′,*N*′′-pentamethyldiethylenetriamine in the presence of triphenylborane and tris(pentafluorophenyl)borane.

Introduction

Molecular zinc compounds have received prominence as reagents for the reduction of unsaturated bonds.[1–4] They are employed in the reduction of olefins,[5–8] imines,[9–11] aldehydes, ketones,[12–18] and carbon dioxide.[19–30] Catalytic reduction of carbon dioxide through catalytic hydrosilylation[31–34] and, to some extent, hydroboration[35,36] with zinc catalysts has been investigated.[37–44] Zinc acetate is known to hydrosilylate CO_2 to a mixture of reduced products: silyl formates, bis(silyl) acetals, methoxysilanes, and methane.[45] The emergence of neutral and cationic molecular zinc alkyls and hydrides have provided more options for CO_2 hydrosilylation. Due to inherent Lewis acidity, alkyl zinc cations promote CO_2 hydrosilylation through activation of the C=O bond. Recent investigations have shown that zinc hydrides catalyze CO_2 hydrosilylation, resulting in selective reduction to silyl formates or methoxysilanes.[43,46] Mechanistic studies have revealed that molecular zinc hydrides insert CO_2 across Zn–H bond. The resulting formate Zn–OC(H)O reacts with the hydrosilane through σ-bond metathesis involving Zn–O and Si–H bonds, regenerating the zinc hydride catalyst accompanied by the displacement of silyl formate.[47] Further studies have revealed that Lewis acid additives, such as $B(C_6F_5)_3$, if introduced in these catalytic reactions, promote the reduction of silyl formates to silyl acetals and eventually to methane.[38] Although these studies provide basic knowledge of the elementary steps, there is ample opportunity to explore the essential role and limits of the Zn–H species and the Lewis acid additives in CO_2 reduction. Our preliminary investigations on a cationic zinc hydride, $[(Me_6tren)ZnH]^+$ (Me_6tren = tris[2-(dimethylamino)ethyl]amine), for CO_2 hydrosilylation in the presence of BPh_3 prompted us to explore the elementary reactions in detail.[48] Herein, we provide new insights into CO_2 hydrosilylation and hydroboration catalyzed by cationic Zn–H moieties. We show the effect of decreased coordination number, resulting in the increased efficiency of hydrosilylation. The effect of the Lewis acids $B(C_6F_5)_3$ and BPh_3 as additives are also explored.

Results and Discussion

We recently reported that $[(Me_6tren)ZnH][B\{3,5\text{-}C_6H_3(CF_3)_2\}_4]$ (**1a**) catalyzed the reaction between CO_2 and $PhSiH_3$ in acetonitrile at 50 °C, resulting in $PhSi(OCHO)_3$ with a conversion of 95% in 2 h (Scheme 1).[48] The Lewis acid BPh_3 was used as an additive in equimolar quantity with respect to the zinc catalyst. The conversion rates were temperature dependent, with the

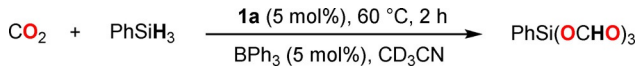

Scheme 1. CO_2 hydrosilylation catalyzed by compound **1a** in the presence of BPh_3.

[a] R. Chambenahalli, R. M. Bhargav, A. P. Andrews, Dr. A. Venugopal
School of Chemistry, Indian Institute of Science Education and Research Thiruvananthapuram, Vithura, Thiruvananthapuram 695551 (India)
E-mail: venugopal@iisertvm.ac.in

[b] K. N. McCabe, Prof. L. Maron
LPCNO, UMR 5215, Université de Toulouse-CNRS, INSA, UPS
31077 Toulouse (France)
E-mail: maron@irsamc.ups-tlse.fr

[c] F. Ritter, Prof. J. Okuda
Institute of Inorganic Chemistry, RWTH Aachen University
Landoltweg 1, 52056 Aachen (Germany)

Supporting information and the ORCID identification number(s) for the author(s) of this article can be found under: https://doi.org/10.1002/chem.202005392.

© 2021 Wiley-VCH GmbH

rates being faster above 50 °C and lower below this temperature. Various solvents were screened for this transformation. Chlorinated solvents, namely, chloroform and dichloromethane, instantly converted $[Me_6trenZnH]^+$ into $[Me_6trenZnCl]^+$; the latter does not further catalyze the reaction. Due to its ionic nature, compound **1a** is insoluble in hydrocarbon solvents. The reaction was found to proceed only in polar aprotic solvents, such as tetrahydrofuran and acetonitrile, with the efficiency being superior in the latter. After screening various hydrosilane sources, it was observed that $PhSiH_3$ was the only hydrosilane source that was active for this transformation under the given reaction conditions. The possibility of interference from the anion in the zinc hydride catalyst was excluded by performing this reaction with different weakly coordinating anions: $[B(3,5\text{-}C_6H_3Cl_2)_4]^-$, $[B\{3,5\text{-}C_6H_3Cl_2(CF_3)_2\}_4]^-$, and $[B(C_6F_5)_4]^-$.

BPh_3 alone is known to catalyze CO_2 hydrosilylation.[49] We, however, observed that it took 100 h in CD_3CN to consume 90% of $PhSiH_3$ to give a mixture of hydrosilylation products, suggesting the reactivity of BPh_3 in catalyzing CO_2 hydrosilylation is far lower in the absence of **1a** (see the Supporting Information). Performing catalysis with **1a** alone as a catalyst also resulted in 90% conversion of $PhSiH_3$ to the respective silyl formate in 150 h. We then considered using more Lewis acidic $B(C_6F_5)_3$ as an additive in place of BPh_3. Although $B(C_6F_5)_3$ alone does not catalyze the reaction, Parkin and co-workers[38] have successfully used it as an additive in zinc hydride catalyzed CO_2 hydrosilylation. To our surprise, if $B(C_6F_5)_3$ was employed in place of BPh_3 as an additive, the catalytic reaction in Scheme 1 was not observed under the given experimental conditions. These observations infer that the Lewis acid additive does not directly impact catalysis, but rather influences the active catalytic species.

Having fixed the reaction conditions, we set out to perform a series of elementary reactions. To understand the role of the Lewis acid additive, equimolar quantities of **1a** and BPh_3 were dissolved in CD_3CN. No reaction was observed, even with prolonged heating at 60 °C. However, the treatment of **1a** with $B(C_6F_5)_3$ in CD_3CN instantaneously led to the abstraction of the hydride from the zinc center, resulting in $[(Me_6tren)Zn(CD_3CN)][HB(C_6F_5)_3][B\{C_6H_3(CF_3)_2\}_4]$, which was further confirmed by performing the reaction in tetrahydrofuran, leading to $[(Me_6tren)Zn(C_4H_8O)][HB(C_6F_5)_3][B\{C_6H_3(CF_3)_2\}_4]$ (**2a**; Scheme 2). The disappearance of the Zn–H signal in the ^1H NMR spectrum and the appearance of a characteristic doublet for $[HB(C_6F_5)_3]^-$ in the ^{11}B NMR spectrum at $\delta = -25.2$ ppm, with a coupling constant of 75 Hz, confirmed the abstraction of hydride in **1a** by $B(C_6F_5)_3$. Compound **2a** was characterized by means of multinuclear NMR spectroscopy and elemental analysis.

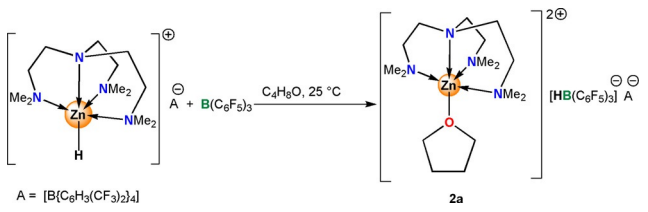

Scheme 2. Hydride abstraction from **1a** with $B(C_6F_5)_3$.

Unlike $B(C_6F_5)_3$, the inability of BPh_3 to abstract the hydride from **1a** can be reasoned based on their Lewis acid strengths. To find experimental evidence for this interpretation, we aimed to quantify and compare the Lewis acidities of BPh_3 and $B(C_6F_5)_3$ with dicationic **2a** by using the Gutmann–Beckett method.[50,51] Accordingly, one equivalent of triethylphosphine oxide (TEPO) was added to solutions of **2a**, BPh_3, and $B(C_6F_5)_3$ in CD_2Cl_2, and the ^{31}P NMR spectra of the resulting solutions were recorded (Figure 1). A chemical shift value of $\delta = 71$ ppm was observed in the case of **2a**, whereas shifts of $\delta = 73.2$ and 77.2 ppm were observed for BPh_3 and $B(C_6F_5)_3$, respectively. These observations suggest that **2a** and BPh_3 possess comparable Lewis acidity, and hence, the hydride cannot be easily abstracted from the zinc center. However, $B(C_6F_5)_3$ has significantly higher Lewis acidity relative to dicationic **2a**, and hence, hydride abstraction from the zinc center in **1a** readily takes place.

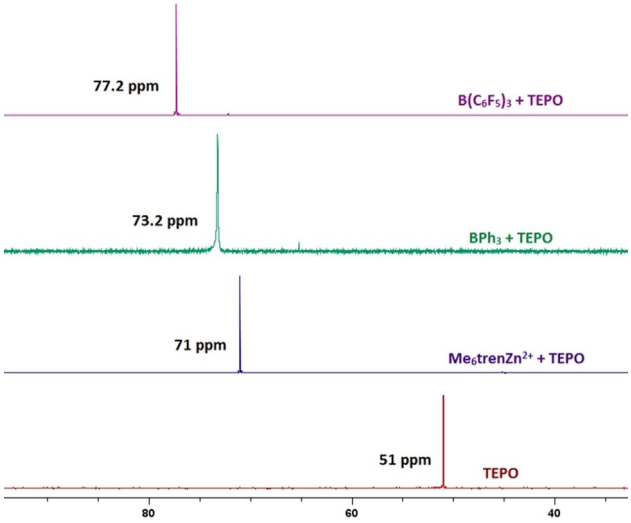

Figure 1. Stacked ^{31}P NMR spectra of TEPO and TEPO with compound **2**, BPh_3, and $B(C_6F_5)_3$.

In our previous investigations, we have established that **1a** readily reacts with CO_2, resulting in the quantitative formation of the zinc formate species, $[(Me_6tren)ZnOCHO][B\{C_6H_3(CF_3)_2\}_4]$ (**3a**). Based on this observation, we proceeded to investigate the reaction between **1a** and CO_2 in the presence of BPh_3. An equimolar mixture of **1a** and BPh_3 in CD_3CN was pressurized with 1 bar of CO_2 to obtain $[(Me_6tren)ZnOCHOBPh_3][B\{C_6H_3(CF_3)_2\}_4]$ (**4a**) instantaneously (Scheme 3). Compound **4a** could be independently prepared by treating zinc formate species **3a** with an equimolar amount of BPh_3 (Scheme 3). The structure of the cationic part in **4a** was confirmed by preparing $[(Me_6tren)ZnOCHOBPh_3][B\{C_6F_5\}_4]$ (**4b**) through a method analogous to that of the synthesis of **4a**. Single crystals of **4b** were grown from a solution in diethyl ether, and X-ray diffraction studies elucidated the solid-state structure (Figure 2).

© 2021 Wiley-VCH GmbH

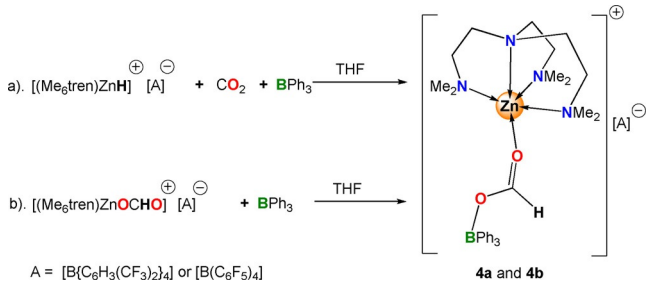

Scheme 3. a) Reactivity of compound **1** with CO_2 and BPh_3. b) Reactivity of compound **3** with BPh_3.

Table 1. Selected bond lengths [Å] of compounds **3a** (citation), **4b**, and **5b**.

	3a	4b	5b
Zn1–N1	2.239(10)	2.181(3)	2.176(2)
Zn1–N2	2.175(11)	2.136(3)	2.120(2)
Zn1–N3	2.151(10)	2.099(3)	2.111(2)
Zn1–N4	2.150(9)	2.085(3)	2.106(2)
Zn1–O1	1.969(9)	2.033(3)	2.0393(18)
C1–O1	1.272(11)	1.240(4)	1.231(3)
C1–O2	1.221(12)	1.264(4)	1.277(3)
B1–O2	–	1.607(2)	1.557(3)

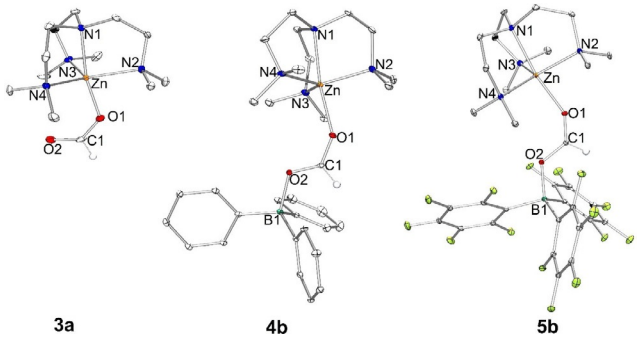

Figure 2. Solid-state structures of cationic parts of **3a**,[48] **4b**, and **5b**. Hydrogen atoms, except H1, are omitted for clarity.

If **1a** was treated with CO_2 in CD_3CN in the presence of $B(C_6F_5)_3$, we observed the abstraction of the hydride from the zinc center by $B(C_6F_5)_3$, resulting in $[(Me_6tren)Zn(solvent)][HB(C_6F_5)_3][B\{C_6H_3(CF_3)_2\}_4]$, and no further reduction of CO_2 was observed under the given conditions (Scheme 4). This observation explains why CO_2 hydrosilylation does not proceed with $B(C_6F_5)_3$ as an additive. However, the zinc formate, **3b**, reacts with $B(C_6F_5)_3$, resulting in $[(Me_6tren)ZnOCHOB(C_6F_5)_3][B(C_6F_5)_4]$ (**5b**). Single-crystal (SC) XRD studies established the structure of **5b** (Figure 2). Examining the bond lengths in **4b** and **5b** (Table 1) shows that Lewis acid binding to the formate oxygen elongates the Zn–O bond from 1.969 to 2.033 Å in the case of BPh_3 and 2.039 Å in the case of $B(C_6F_5)_3$. This elongation is proportional to the strength of the Lewis acid.

Having obtained the formate adducts, **4b** and **5b**, of the Lewis acids, we tested their reactivity with $PhSiH_3$ in CD_3CN. Although **4b** reacted with $PhSiH_3$ to displace $PhSiH_2(OCHO)$ and regenerate the zinc hydride catalyst, $[(Me_6tren)ZnH][B(C_6F_5)_4]$ (**1b**). Compound **5b** reacted with $PhSiH_3$, resulting in $PhSiH_2(OCHO)$, and the dicationic zinc compound, $[Me_6trenZn(CD_3CN)][HB(C_6F_5)_3][B(C_6F_5)_4]$ (Scheme 4). From the above observations, we concluded that the use of BPh_3 along with **1b** resulted in the catalytic conversion of CO_2 to $PhSi(OCHO)_3$, whereas employing $B(C_6F_5)_3$ with **1b** resulted in the stoichiometric conversion of CO_2 into $PhSiH_2(OCHO)$. Having explored the elementary reactions (Scheme 5) in CO_2 hydrosilylation mediated by **1a** and **1b**, we concluded that BPh_3 was the desired additive over $B(C_6F_5)_3$. However, the exact role of the former Lewis acid remained unexplained. We thus resorted to computations to re-explore the elementary reactions in the catalytic cycle.

Calculations were carried out on the reaction mechanism of CO_2 hydrosilylation with $PhSiH_3$ catalyzed by **1** in the presence of BPh_3 at the DFT level (B3PW91; see the Supporting Information for computational details). The initial step involves the Zn–H moiety (**A**) inserting CO_2 via a four-membered transition state (I) with an activation barrier of 14.3 kcal mol^{-1}, resulting in a monomeric zinc formate species, **B** (Figure 3). With a moderate energy gain of 3.5 kcal mol^{-1}, species **B** can dimerize to **C**. Dimeric **C** is broken down with BPh_3, resulting in **D**, and this step is exothermic by 33.1 kcal mol^{-1}. We ruled out the possibility of silane-assisted dimer cleavage, since the induced stabilization is only 12.6 kcal mol^{-1} (see the Supporting Information). Species **D** then interacts with a silane molecule, leading to four-membered σ-bond metathesis, with an associated barrier of 18.1 kcal mol^{-1}. The transition state (II) appears to be favored due to the coordination of BPh_3 to the carbonyl oxygen

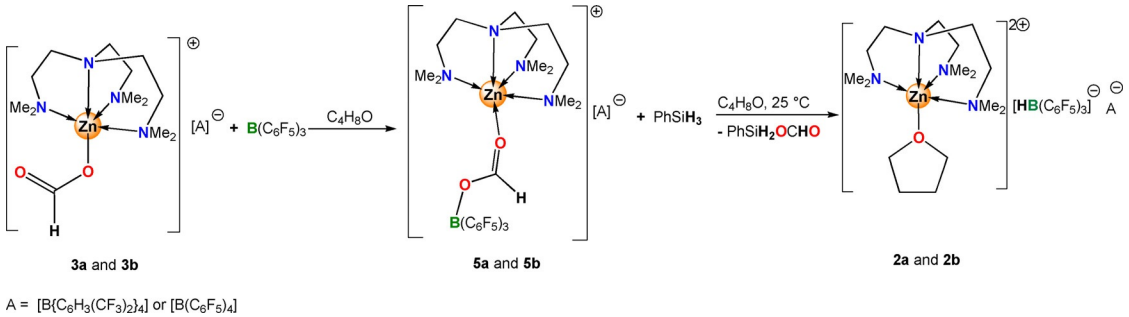

Scheme 4. Stoichiometric reactions of compound **3** with $B(C_6F_5)_3$ and **5** with $PhSiH_3$.

© 2021 Wiley-VCH GmbH

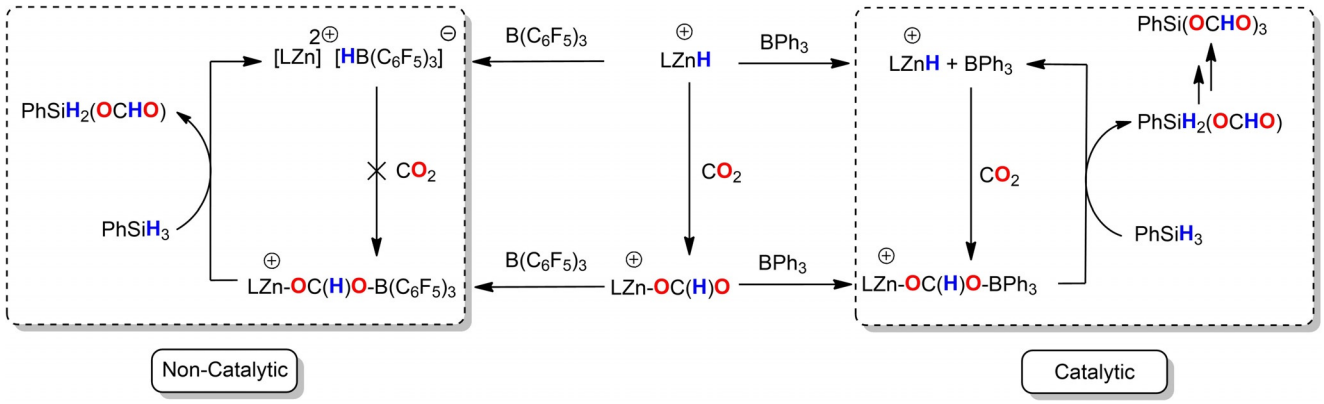

Scheme 5. Schematic representation of the effect of Lewis acids on **1** and **3** in CO_2 hydrosilylation.

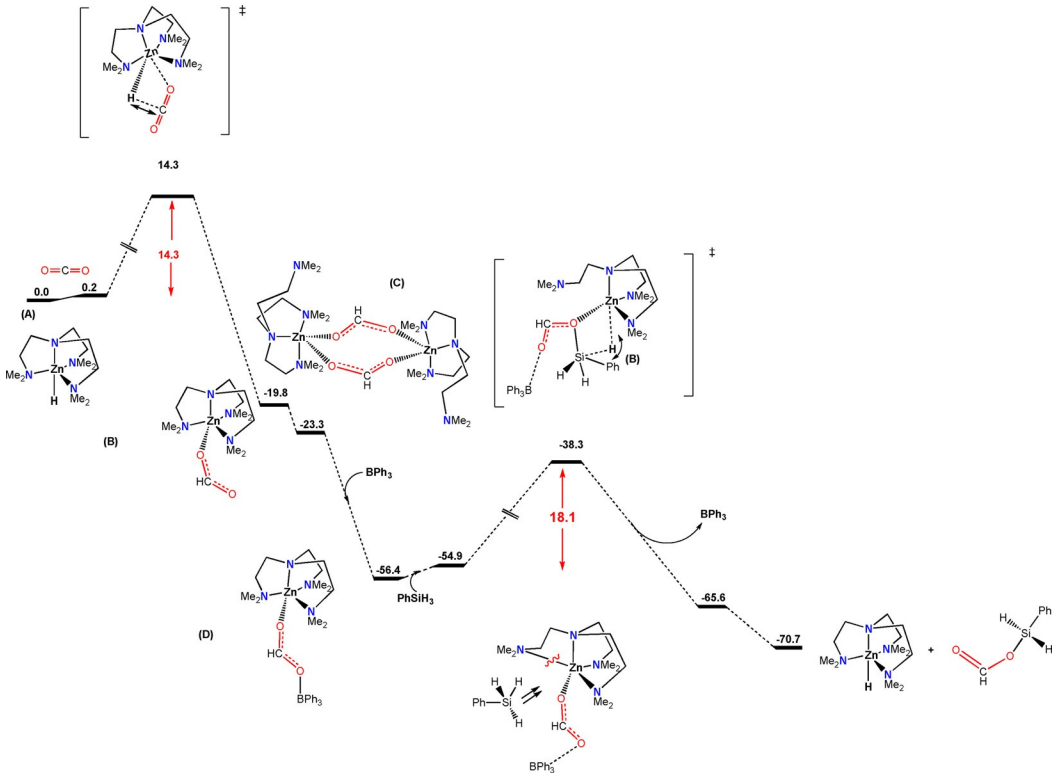

Figure 3. Computed enthalpy profile for the hydrosilylation of CO_2 catalyzed by **1** in the presence of BPh_3.

(see Figures S54 and S55 in the Supporting Information). Following the intrinsic reaction coordinate, silyl formate is obtained, along with the regeneration of the zinc hydride catalyst. The overall cycle is an exothermic reaction by 70.7 kcal mol^{-1}. From the reaction profile, it is proposed that silane activation is the rate-determining step. Interestingly enough, hydrosilylation appears to be an endothermic reaction in the absence of BPh_3 because of the formation of a very stable (μ-κ2-O,O) formate intermediate **C**.

We could not obtain conclusive experimental evidence for the existence of compound **3** as a dimer in solution. Variable-temperature NMR spectroscopy studies on **3** did not provide evidence to prove the dimeric form in solution. To address this issue, we then set out to prepare a cationic zinc hydride with a decreased coordination number by using the tridentate *N*,*N*,*N*′,*N*′′,*N*′′-pentamethyldiethylenetriamine (PMDTA). [(pmdta)ZnEt][$B(C_6F_5)_4$] (**6**) was employed as a precursor to access [(pmdta)$ZnOSiPh_3$][$B(C_6F_5)_4$] (**7**), which was then treated with excess $PhSiH_3$ to obtain [(pmdta)ZnH][$B(C_6F_5)_4$] (**8**; Scheme 6). In another method, the treatment of polymeric ZnH_2 with Brønsted acid [(pmdta)H][$B(C_6F_5)_4$] also led to the formation of **8** (Scheme 6). Compounds **6**–**8** were characterized by means of multinuclear NMR spectroscopic studies, elemental analysis, and SC-XRD studies (Figure 4). The ^{1}H NMR spectrum of [(pmdta)ZnH][$B(3,5\text{-}Me_2\text{-}C_6H_3)_4$] (**8b**) recorded in [$D_8$]THF shows a characteristic Zn–H signal at $\delta = 3.41$ ppm. SC-XRD studies revealed that **8** had a tetrahedral coordination geometry at zinc with three sites occupied by the three nitro-

© 2021 Wiley-VCH GmbH

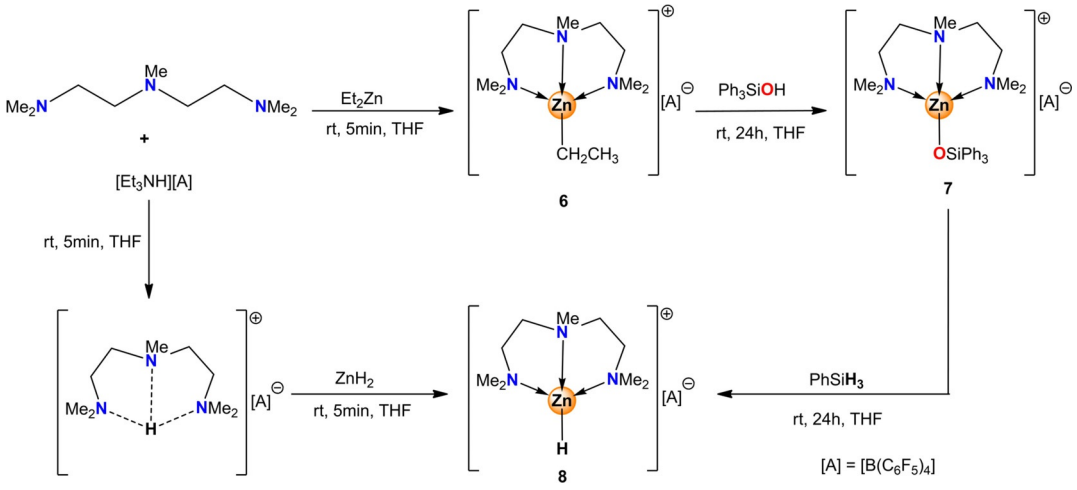

Scheme 6. Synthesis of compounds **6**, **7**, and **8**.

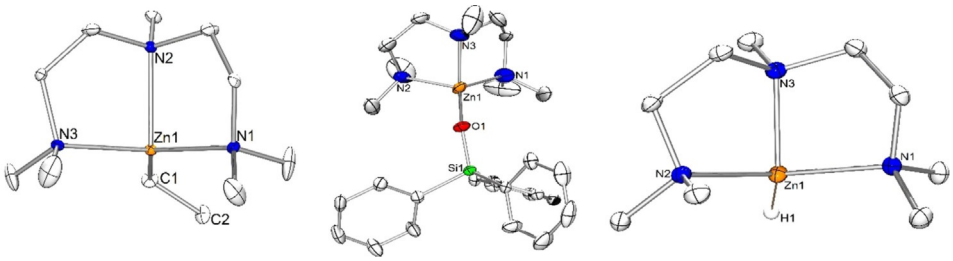

Figure 4. Solid-state structures of the cationic parts of **6**, **7**, and **8**. Hydrogen atoms, except H1, in **8** are omitted for clarity.

gen atoms of PMDTA and the fourth corner occupied by a hydrogen atom with a Zn–H distance of 1.469 Å (Figure 4). IR spectroscopic studies provided a characteristic Zn–H stretching frequency at 1765 cm^{-1} (see the Supporting Information).

Compound **8** was pressurized with 1 bar of CO_2 to form [(pmdta)ZnOCHO][$B(C_6F_5)_4$] (**9**) (Scheme 7). The ^1H NMR spectrum of **9** recorded in CD_3CN shows a single signal for the formate C–H at $\delta = 8.22$ ppm, and the respective carbon shows a single sharp signal at $\delta = 169.6$ ppm in the ^{13}C NMR spectrum (see the Supporting Information). Crystallographic studies revealed that the cationic moiety in **9** existed as a dimer in the solid state, with a distorted trigonal bipyramidal coordination geometry at the zinc center (Figure 5). The central zinc metal is coordinated to three nitrogen atoms of PMDTA, with an average Zn–N distance of 2.129 Å, and two oxygen atoms with Zn–O distances of 1.966 and 2.085 Å (Figure 5). Treatment of

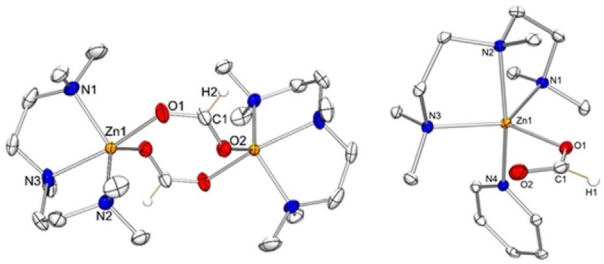

Figure 5. Solid-state structures of the cationic parts of **9** and **10**. Hydrogen atoms, except H1 and H2, are omitted for clarity.

the dimeric formate complex with pyridine (py) resulted in the formation of a mononuclear complex [(pmdta)ZnOCHO(py)][A] (**10**), which was characterized by means of SC-XRD and found

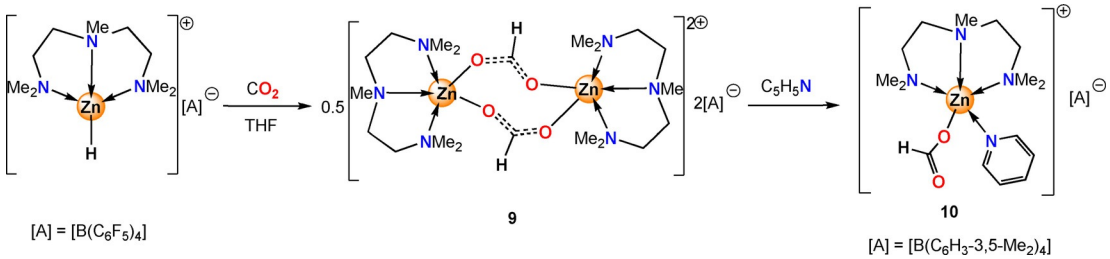

Scheme 7. Synthesis of compounds **9** and **10**.

© 2021 Wiley-VCH GmbH

to contain a five-coordinate zinc center for A = $B(C_6H_3$-2,5-$Me_2)_4$.

Furthermore, compound **9** was treated with two equivalents of BPh_3 and $B(C_6F_5)_3$. Similar observations were made to those observed for **3** to form [(pmdta)ZnOCHOBPh_3][$B(C_6F_5)_4$] (**11**) and [(pmdta)ZnOCHOB$(C_6F_5)_3$][$B(C_6F_5)_4$] (**12**). Compound **12**, upon treatment with an excess of $PhSiH_3$ in CD_3CN, resulted in [(pmdta)Zn(CD_3CN)][$HB(C_6F_5)_3$][$B(C_6F_5)_4$] (**13**). Compounds **10**–**12** were formed in situ in CD_3CN and the structures were confirmed by means of multinuclear NMR spectroscopy studies. These observations suggest that the decreased denticity of the ancillary ligand stabilizes the dimeric form of the zinc formate species. Hence, energy has to be supplied externally to break the dimer and facilitate hydrosilylation.

Before proceeding to catalytic experiments, theoretical investigations were performed on the hydrosilylation of CO_2 catalyzed by **8** (Figure 6). The reaction mechanism is very similar to that of **A** depicted in the reaction profile in Figure 3, and hence, only the main differences between the two are discussed. The activation barrier for CO_2 reduction to formate by **E** is 17.7 kcal mol^{-1}, which is slightly higher than that for **A** (14.3 kcal mol^{-1}). This is mainly due to the greater electronic deficiency of the zinc center in **E** than that in **A**, as proven by the zinc charges (+1.78 in **E** vs. +1.54 in **A**, whereas the charges of the hydrides are −0.58 in **E** and −0.34 in **A**). Although the formation of monomeric formate (**F**) is exothermic (−0.7 kcal mol^{-1}), dimerization is favored (−13.0 kcal mol^{-1}), resulting in dimer **G**, in agreement with experimental observations. The coordination of BPh_3 allows cleavage of the dimer to form **H**, which undergoes hydrosilylation with an associated barrier of 16.2 kcal mol^{-1}, indicating that CO_2 insertion is the rate-determining step of the reaction. Moreover, the highest barrier in the process is slightly lower for compound **8** than that for compound **1** (17.7 vs. 18.1 kcal mol^{-1}), so that compound **8** can be considered more active than that of **1**.

The above studies prompted us to perform catalytic hydrosilylation of CO_2 with compound **8**. As expected, compound **8** alone did not catalyze CO_2 hydrosilylation in CD_3CN at 60 °C, even after 2 d. However, compound **8** and equimolar molar amounts of BPh_3 (1 mol% each) catalyzed the reaction between CO_2 (1.5 bar) and $PhSiH_3$ in CD_3CN, resulting in 90% conversion of Si–H into Si–OCHO. We further observed that Ph_2SiH_2, which did not hydrosilylate CO_2 in the presence of **1** and BPh_3, reacted with CO_2 in the presence of catalytic amounts of **8** and BPh_3. This observation proves that **8** is more efficient than the reaction with **1** in the presence of BPh_3. We also observed that a combination of **8** and $B(C_6F_5)_3$ did not catalyze the hydrosilylation of CO_2 under similar conditions and even at 75 °C.

To experimentally prove that the role of BPh_3, as explained theoretically, is to break the formed dimers of compounds **3** and **9**, further experiments have been considered. We performed the hydroboration of CO_2 by using **3** and **9** as catalysts in the presence of bis(pinacolato)diboron (Hbpin; Scheme 8), which is expected to play the dual role of serving as a Lewis acidic center to facilitate monomeric catalyst formation and as

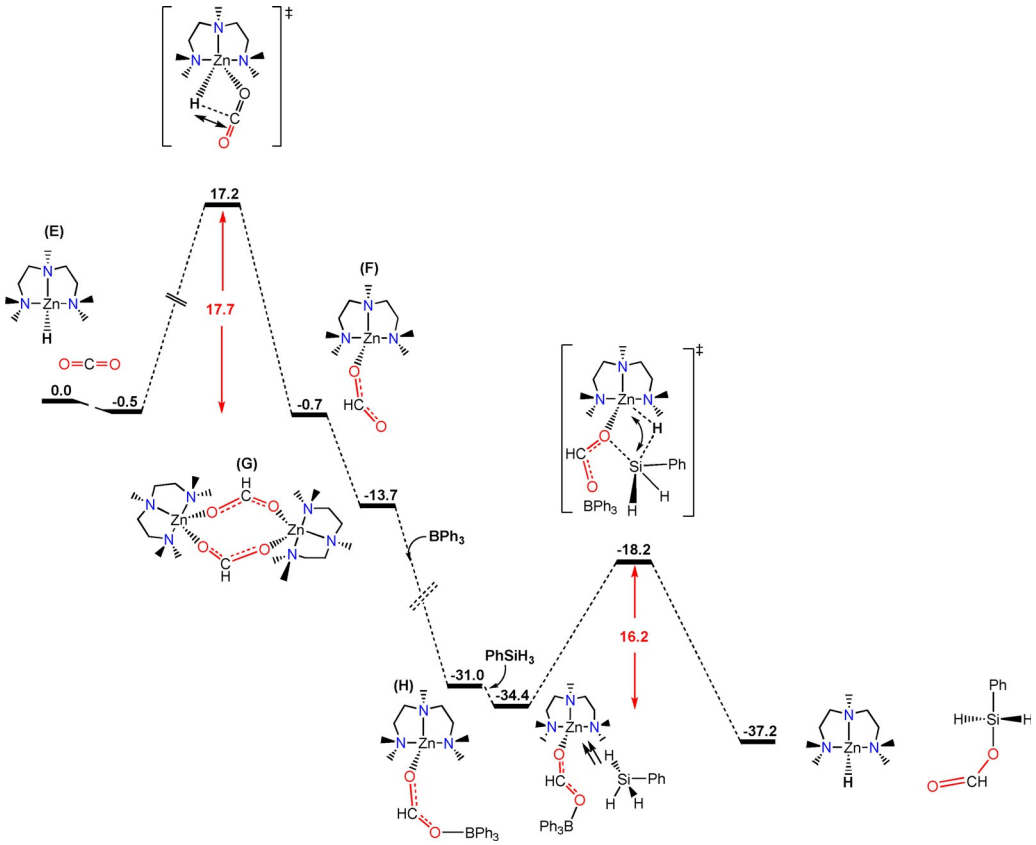

Figure 6. Computed enthalpy profile for the hydrosilylation of CO_2 catalyzed by **8** in the presence of BPh_3.

© 2021 Wiley-VCH GmbH

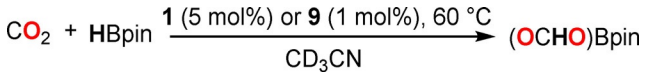

Scheme 8. CO_2 hydroboration catalyzed by compounds **1** and **9**.

a hydride transfer reagent. Whereas 5 mol% of **3** catalyzed the hydroboration of CO_2 selectively to OCHOBpin in 2 h at 60 °C, a decreased catalyst loading of 1 mol% was required in the case of **9**. Computational studies revealed that this reaction proceeded via a six-membered transition state involving Zn–OC(H)–O and HBpin, with an activation barrier of 5.6 kcal mol^{-1} (Figure 7).

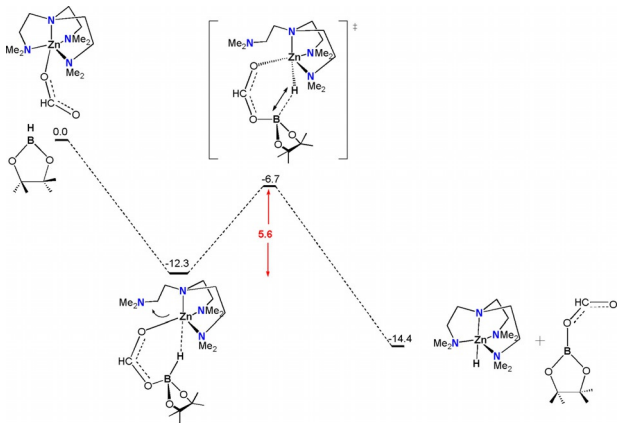

Figure 7. Computed enthalpy profile for the hydroboration of CO_2 catalyzed by compound **3**.

Comparative data on catalytic CO_2 hydrosilylation and hydroboration by compounds **1** and **8** are given in Table 2. Compound **8** in the presence of BPh_3 gives the highest TON of 273 with a TOF of 136.49 h^{-1}, in comparison with previously reported compound **1**. This TOF is, so far, the best value observed in the case of molecular zinc compounds.[46] It was also observed that, in the absence of BPh_3, compound **8** did not catalyze CO_2 hydrosilylation, whereas compound **1** does, with a TON of 18 and TOF of 0.12 h^{-1}. Compound **2** did not play any role in CO_2 hydrosilylation either in the presence of compound **1** or on its own. Hydroboration was catalyzed by both compounds **1** and **8**, which did not necessitate the addition of Lewis acids. Compound **8** also proved to be a better catalyst for hydroboration of CO_2 with TON and TOF values of 94 and 42 h^{-1}, respectively.

Conclusion

Experiments and DFT calculations on $[(Me_6tren)ZnH]^+$ and $[(pmdta)ZnH]^+$ have provided crucial evidence to understand the elementary reactions operative in CO_2 reduction catalyzed by cationic zinc hydrides. The isolation of key intermediates has re-enforced the theoretical propositions on the catalytic cycles. Five-coordinate $[(Me_6tren)ZnH]^+$ alone shows moderate reactivity towards CO_2 hydrosilylation. Although decreased ligand denticity is expected to exhibit higher reactivity, four-coordinate $[(pmdta)ZnH]^+$ alone did not catalyze this process. This has been attributed to the formation of a stable zinc formate dimer. The mild Lewis acid BPh_3 was employed as an additive to generate the monomeric zinc formate to facilitate hydrosilylation. $B(C_6F_5)_3$ is an attractive choice as a strong Lewis acid additive, but we have observed that it arrests the catalytic cycle by the formation a stable $[HB(C_6F_5)_3]^-$ anion. The use of the hydroboration reagent HBpin further strengthened our proposition of the role of the secondary Lewis acid in cationic zinc hydride mediated CO_2 reduction. Our findings validate the role of cationic zinc centers in the activation of Si–H and B–H bonds and reveal the importance of the second Lewis acidic center for facile catalytic CO_2 reduction.

Experimental Section

General

All reactions were performed under an argon atmosphere by using standard Schlenk techniques or in a glove box under an argon atmosphere. Before use, glassware was dried at 200 °C, and solvents were dried, distilled, and degassed by using standard methods.[52,53] Me_6tren,[54] $[HNEt_3][B\{C_6H_3(CF_3)_2\}_4]$, $[(Me_6tren)ZnH][A]$, and $[(Me_6tren)ZnOCHO][A]$ ($A = B(C_6H_3(CF_3)_2)_4/B(C_6F_5)_4$) were synthesized and purified according to procedures reported in the literature.[48] $ZnEt_2$ was purchased from Sigma and used as received. $[ZnH_2]_n$, $[HNEt_3][B(3,5\text{-}(CF_3)_2C_6H_3)_4]$, and $[HNEt_3][B(3,5\text{-}(CF_3)_2C_6H_3)_4]$ ($[HNEt_3][B(C_6F_5)_4]$) were synthesized according to procedures reported in

Table 2. Comparative data on catalytic CO_2 hydrosilylation and hydroboration.[a]

Entry	Catalyst[b] ([mol%])	Additive ([mol%])	Hydride source	T [°C]	t [h]	Conversion [%]	TON[c]	TOF[d] [h^{-1}]
1	**8a/b** (5)	–	$PhSiH_3$	60	24	0	0.0	0.00
2	**1a/b** (5)	–	$PhSiH_3$	60	150	90	18.0	0.12
3	**1a/b** (5)	**2** (5)	$PhSiH_3$	60	100	92	18.4	0.18
4	**1a/b** (1.66)	BPh_3 (1.66)	$PhSiH_3$	45	2	98	58.8	29.4[48]
5	**8a/b** (0.33)	BPh_3 (0.33)	$PhSiH_3$	60	2	91	273.0	136.49
6	**1a/b** (5)	–	Ph_2SiH_2	60	24	0	0.0	0
7	**8a/b** (5)	–	Ph_2SiH_2	60	24	0	0.0	0
8	**8a/b** (5)	BPh_3 (5)	Ph_2SiH_2	60–75	24	98	19.6	0.82
9	**1a/b** (5)	–	HBpin	60	6	95	19	3.16
10	**8a/b** (1)	–	HBpin	60	2	94	94	42.00

[a] A constant pressure of 1.5 bar of CO_2 was maintained during catalysis. [b] With respect to Si–H. [c] TON = turnover number. [d] TOF = turnover frequency.

© 2021 Wiley-VCH GmbH

the literature.[55–57] BPh_3 and $B(C_6F_5)_3$ were purchased from Sigma–Aldrich and purified by sublimation prior to use. PMDTA, $PhSiH_3$, Ph_2SiH_2, and Et_3SiH were purchased from TCI Chemicals and distilled before use. Ph_3SiOH was purchased from Sigma–Aldrich, purified by recrystallization, and dried in vacuo before use. CO_2 (99.990% purity) was purchased from commercial sources. The gases were passed through a column of molecular sieves dried overnight at 200 °C before performing the reactions by using Schlenk manifolds. ^1H, ^{13}C, ^{11}B, and ^{19}F NMR spectra were recorded on a Bruker 500 MHz and DRX400 spectrometers. Chemical shifts (δ, in ppm) in the ^1H and ^{13}C NMR spectra were referenced to the residual signals of the deuterated solvents. ^{11}B NMR spectra were referenced to the $NaBH_4$ signal in D_2O. ^{19}F NMR spectra were referenced to the $CFCl_3$ signal. Abbreviations for NMR spectra: s (singlet), d (doublet), t (triplet), q (quartet), quin (quintuplet), sext (sextet), sep (septet), and br (broad). Samples for elemental analysis were rigorously dried in vacuo at 10^{-3} mbar pressure. IR spectra were recorded as KBr pellets by using AVATAR 360 FTIR and Prestige-21 SHIMADZU FTIR spectrometers. Elemental analyses were performed on an Elemental Vario Micro Cube machine. Crystals were suspended in paraffin oil before being mounted on the X-ray diffractometer. XRD data were collected on a Bruker Kappa Apex-II charge-coupled device (CCD) diffractometer at 150 K and with $Mo_{K\alpha}$ irradiation ($\lambda = 0.71073$ Å). SC-XRD data for **4b**, **5b**, **6b**, **7**, **8a**, **8b**, **9a**, **10b**, and **10c** are reported in crystallographic information files (CIF) accompanying this document. Details on data collection, reduction, and refinement can be found in the individual CIFs.

Synthesis of 2b

A solution of $B(C_6F_5)_3$ (0.086 mmol, 0.047 g) in THF (2 mL) was slowly added to a solution of compound **1b** (0.086 mmol, 0.100 g) in THF (2 mL). The reaction mixture was stirred for 30 s. Volatile compounds were removed under vacuum, followed by washing the residue with pentane, yielding the product as an off-white powder (0.130 g, 87%). ^1H NMR (CD_3CN, 500 MHz): $\delta = 2.53$ (s, 18H; NCH_3), 2.75 (t, $^3J(H,H) = 5$ Hz, 6H; NCH_2), 2.88 (t, $^3J(H,H) = 5$ Hz, 6H; NCH_2), 8.09 ppm (s, OCHO); $^{13}C\{^1H\}$ NMR (CD_3CN, 126 MHz): $\delta = 47.5$ (NCH_3), 49.8 (NCH_2), 57.3 (NCH2), 136.4 (*i*-C, C_6F_5), 138.3 (*p*-C, C_6F_5), 148.2 (*m*-C, C_6F_5), 150.0 (*o*-C, C_6F_5), 164.9 ppm (s, OCHO) (Figure S6 in the Supporting Information); ^{11}B NMR (CD_3CN, 128 MHz): $\delta = -16.7$ (s, $B(C_6F_5)_4$), −4.4 ppm (br, $OBPh_3$); ^{19}F NMR (CD_3CN, 471 MHz): $\delta = -133.76$ (*o*-*CF*), −163.94 (*p*-*CF*), −168.36 ppm (*m*-*CF*); satisfactory elemental analysis values for CHN could not be obtained for this compound due the presence of trace amounts of solvent molecules.

Synthesis of 4b

Method A: Compound **1b** (0.102 mmol, 0.100 g) and BPh_3 (0.102 mmol, 0.025 g) in THF (5 mL) were pressurized with dry CO_2 (1 bar). The reaction mixture was stirred at room temperature for 10 min. The volatile compounds were evaporated under vacuum (10^{-3} mbar) at room temperature to give **4b** as a colorless powder. Compound **4b** was further purified by recrystallization at 25 °C in diethyl ether upon *n*-pentane layering (0.112 g, 85%).

Method B: A solution of BPh_3 (0.098 mmol, 0.023 g) in THF (2 mL) was slowly added to a solution of compound **3b** (0.0980 mmol, 0.100 g) in THF (2 mL). The reaction mixture was stirred at room temperature for 5 min. All volatile compounds were evaporated under vacuum (10^{-3} mbar) at room temperature to give **4b** as a colorless powder. Compound **4b** was further purified by recrystallization at 25 °C in diethyl ether upon *n*-pentane layering (0.108 g, 89%). ^1H NMR (CD_3CN, 500 MHz): $\delta = 2.50$ (s, 18H; NCH_3), 2.68 (t, $^3J(H,H) = 5$ Hz, 6H; NCH_2), 2.84 (t, $^3J(H,H) = 5$ Hz, 6H; NCH_2), 7.08 (m, 3H; *p*-C_6H_5), 7.17 (m, 6H; *m*-C_6H_5), 7.24 (m, 6H; *o*-C_6H_5), 8.44 ppm (s, 1H; OCHO); $^{13}C\{^1H\}$ NMR (CD_3CN, 126 MHz): $\delta = 47.4$ (NCH_3), 50.4 (NCH_2), 57.2 (NCH2), 125.8 (*p*-C, C_6H_5), 127.8 (*m*-C, C_6H_5), 134.1 (*o*-C, C_6H_5), 136.4 (*i*-C, C_6F_5), 138.3 (*p*-C, C_6F_5), 148.1 (*m*-C, C_6F_5), 150.0 (*o*-C, C_6F_5), 169.1 ppm (s, OCHO); ^{11}B NMR (CD_3CN, 128 MHz): $\delta -16.7$ (s, $B(C_6F_5)_4$), 2.5 ppm (br, $OBPh_3$); ^{19}F NMR (CD_3CN, 471 MHz): $\delta -133.76$ (*o*-*CF*), −163.94 (*p*-*CF*), −168.36 ppm (*m*-*CF*); elemental analysis calcd (%) for $C_{55}H_{46}B_2F_{20}N_4O_2Zn$: C 52.35, H 3.67, N 4.44: found: C 52.24, H 3.60, N 4.40.

Synthesis of 5b

A solution of $B(C_6F_5)_3$ (0.098 mmol, 0.050 g) in THF (2 mL) was slowly added to the solution of compound **3b** (0.098 mmol, 0.100 g) in diethyl ether (2 mL). The reaction mixture was stirred for 2 min and further concentrated to about 2 mL and layered with *n*-pentane at room temperature to give **5b** as colorless crystals in 24 h (0.130 g, 87%). ^1H NMR (CD_3CN, 500 MHz): $\delta = 2.53$ (s, 18H; NCH_3), 2.75 (t, $^3J(H,H) = 5$ Hz, 6H; NCH_2), 2.88 (t, $^3J(H,H) = 5$ Hz, 6H; NCH_2), 8.09 ppm (s, 1H; OCHO); $^{13}C\{^1H\}$ NMR (CD_3CN, 126 MHz): $\delta = 47.5$ (NCH_3), 49.8 (NCH_2), 57.3 (NCH2), 136.4 (*i*-C, C_6F_5), 138.3 (*p*-C, C_6F_5), 148.2 (*m*-C, C_6F_5), 150.0 (*o*-C, C_6F_5), 164.9 ppm (s, OCHO); ^{11}B NMR (CD_3CN, 128 MHz): $\delta = -16.7$ (s, $B(C_6F_5)_4$), −4.4 ppm (br, $OBPh_3$); ^{19}F NMR (CD_3CN, 471 MHz): $\delta = -133.76$ (*o*-*CF*), −163.94 (*p*-*CF*), −168.36 ppm (*m*-*CF*); elemental analysis calcd (%) for $C_{55}H_{31}B_2F_{35}N_4O_2Zn$: C 43.12, H 2.04, N 3.66; found: C 43.00, H 1.99, N 3.60.

Synthesis of 6a

$[Et_3NH][B(C_6F_5)_4]$ (0.48 mmol, 0.383 g) was added to a solution of PMDTA (0.48 mmol, 0.100 mL) in diethyl ether (2 mL). The reaction mixture was stirred for 2 min. A 1 M solution of Et_2Zn (0.48 mmol, 0.48 mL) was slowly added to the reaction mixture through a syringe at room temperature then stirred for 1 min. A white solid precipitated out and was filtered subsequently. The residue was dried under vacuum (10^{-3} mbar) at room temperature and washed with pentane (5×3 mL) to give **6** as a pale brown powder. Colorless crystals were obtained from the concentrated solution in diethyl ether at −30 °C in 12 h (0.380 g, 85%). Because the crystals were not of good quality, a similar procedure was repeated to give $[(pmdta)ZnEt][B(C_6H_3Cl_2)_4]$ from $[Et_3NH][B(C_6H_3Cl_2)_4]$. Good-quality crystals were grown from a solution in acetonitrile/pentane at room temperature. ^1H NMR (CD_3CN, 500 MHz): $\delta = 0.14$ (q, $^3J(H,H) = 10$ Hz, 2H; CH_2Me_3), 1.20 (t, $^3J(H,H) = 10$ Hz, 3H; CCH_3), 2.50 (s, 12H; NCH_3), 2.58 (s, 3H; NCH_2), 2.74 (m, 4H; NCH_2), 2.83 ppm (m, 4H; NCH_2); $^{13}C\{^1H\}$ NMR (CD_3CN, 126 MHz): $\delta = -3.1$ (CH_2Me), 13.1 (CCH_3), 45.9 (NCH_3), 47.4 ({NCH_3}$_2$), 54.4 (NCH_2), 58.1 (NCH_2), 136.4 (*i*-C, C_6F_5), 138.3 (*p*-C, C_6F_5), 148.2 (*m*-C, C_6F_5), 150.0 ppm (*o*-C, C_6F_5); ^{11}B NMR (CD_3CN, 128 MHz): $\delta = -16.66$ ppm; ^{19}F NMR (CD_3CN, 471 MHz): $\delta = -133.76$ (br s, *o*-*CF*), −163.94 (t, *p*-*CF*), −168.36 ppm (t, *m*-*CF*); elemental analysis calcd (%) for $C_{35}H_{28}BF_{20}N_3Zn$: C 44.40, H 2.98, N 4.44; found: C 44.10, H 3.77, N 4.31.

Synthesis of 7

Compound **6** (0.317 mmol, 0.300 g) and Ph_3SiOH (0.317 mmol, 0.088 g) were taken in THF (5 mL). The reaction mixture was stirred for 20 h at room temperature. All volatile compounds were evaporated under vacuum (10^{-3} mbar) at room temperature, washed twice with *n*-pentane(2×5 mL), and dried to give **7** as a colorless powder, which was further purified by recrystallization at −30 °C in

© 2021 Wiley-VCH GmbH

THF upon *n*-pentane layering (0.425 g, 96%). ^{1}H NMR (CD_3CN, 500 MHz): δ = 2.34 (s, 6H; NCH_3), 2.38 (s, 3H; NCH_3), 2.40 (s, 6H; NCH_3), 2.50 (m, 2H; NCH_2), 2.69 (m, 4H; NCH_2), 2.81 (m, 2H; NCH_2), 7.33 (br m, 9H; *p*-C*H*, *m*-C*H*, C_6H_5), 7.68 ppm (br m, 6H; *o*-C*H*, C_6H_5); ^{13}C{^{1}H} NMR (CD_3CN, 126 MHz): δ = 44.73 (NCH_3), 45.8 ({NCH_3}$_2$), 47.9 ({NCH_3}$_2$), 54.74 (NCH_2), 58.1 (NCH_2), 128.4 (*m*-C, C_6H_5), 129.5 (*p*-C, C_6H_5), 135.9 (*o*-C, C_6H_5), 136.4 (*i*-C, C_6F_5), 138.3 (*p*-C, C_6F_5), 142.8 (*i*-C, C_6H_5), 148.2 (*m*-C, C_6F_5), 150.0 ppm (*o*-C, C_6F_5); ^{11}B NMR (CD_3CN, 128 MHz): δ = −16.66 ppm; ^{19}F NMR (CD_3CN, 471 MHz): δ = −133.76 (br s, *o*-C*F*), −163.94 (t, *p*-C*F*), −168.36 ppm (t, *m*-C*F*); elemental analysis calcd (%) for $C_{51}H_{28}BF_{20}N_3OSiZn$: C 51.34, H 3.21, N 3.52; found: C 51.20, H 3.28, N 3.60;

Synthesis of 8a

$PhSiH_3$ (0.369 mmol, 0.045 mL) was added to a solution of **7** (0.167 mmol, 0.200 g) in THF (5 mL). The reaction mixture was stirred for 24 h at room temperature. Traces of black precipitate formed during the reaction and were removed by filtration. All volatile compounds were removed under vacuum (10^{-3} mbar) at room temperature, washed with *n*-pentane (3×5 mL), and dried to give **8** as a colorless powder. The compound was recrystallized in THF upon layering with *n*-pentane at −30 °C (0.126 g, 82%). ^{1}H NMR (CD_3CN, 500 MHz): δ = 2.34 (s, 6H; NCH_3), 2.38 (s, 3H; NCH_3), 2.40 (s, 6H; NCH_3), 2.50 (m, 2H; NCH_2), 2.69 (m, 4H; NCH_2), 2.81 (m, 2H; NCH_2), 7.33 (br m, 9H; *p*-C*H*, *m*-C*H*, C_6H_5), 7.68 ppm (br m, 6H; *o*-C*H*, C_6H_5); ^{13}C{^{1}H} NMR (CD_3CN, 126 MHz): δ = 44.73 (NCH_3), 45.8 ({NCH_3}$_2$), 47.9 ({NCH_3}$_2$), 54.74 (NCH_2), 58.1 (NCH_2), 128.4 (*m*-C, C_6H_5), 129.5 (*p*-C, C_6H_5), 135.9 (*o*-C, C_6H_5), 136.4 (*i*-C, C_6F_5), 138.3 (*p*-C, C_6F_5), 142.8 (*i*-C, C_6H_5), 148.2 (*m*-C, C_6F_5), 150.0 ppm (*o*-C, C_6F_5); ^{11}B NMR (CD_3CN, 128 MHz): δ−16.66 ppm; ^{19}F NMR (CD_3CN, 471 MHz): δ = −133.76 (br s, *o*-C*F*), −163.94 (t, *p*-C*F*), −168.36 ppm (t, *m*-C*F*); elemental analysis calcd (%) for $C_{33}H_{24}BF_{20}N_3Zn$: C 43.14, H 2.63, N 4.57; found: C 43.02, H 2.55, N 4.50.

Synthesis of 8b

A suspension of $[ZnH_2]_n$ (53 mg, 792 μmol) in THF was added to a solution of [(pmdta)H][B(3,5-Me_2-C_6H_3)] (400 mg, 660 μmol) in THF dropwise at room temperature. After gas evolution ceased (approximately 15 min), the reaction mixture was filtered and the solvent volume was reduced in vacuo. Addition of *n*-pentane resulted in the precipitation of a colorless solid, which was isolated by decantation and subsequently dried under reduced pressure. Compound **8b** was obtained as a colorless solid (421 mg, 627 μmol, 95%). ^{1}H NMR (400 MHz, [D_8]THF): δ = 2.11 (s, 24H; Ar-CH_3), 2.25 (s, 12H; *N*-CH_3), 2.20–2.29 (m, 8H; *N*-CH_2), 2.31 (s, 3H; *N*-CH_3), 3.41 (s, 1H; Zn-*H*), 6.38 (s, 4H; *para*-C_6H_3), 7.01 ppm (s, 8H; *ortho*-C_6H_3); ^{13}C{^{1}H} NMR (101 MHz, [D_8]THF): δ = 22.3 (Ar-CH_3), 45.4 (*N*-CH_3), 47.1 (*N*-CH_3), 54.2 (*N*-CH_2), 57.8 (*N*-CH_2), 123.7 (*para*-C_6H_3), 133.1 (*meta*-C_6H_3), 135.5 (*ortho*-C_6H_3), 165.7 ppm (q, ^1J(B,C) = 49.2 Hz, *ipso*-C_6H_3); ^{11}B{^{1}H} NMR (128 MHz, [D_8]THF): δ = −6.97 ppm; elemental analysis calcd (%) for $C_{41}H_{60}BN_3Zn$: C 73.38, H 9.01, N 6.26; found: C 72.44, H 8.99, N 6.47.

Synthesis of 8c

A suspension of $[ZnH_2]_n$ (53 mg, 792 μmol) in THF was added a solution of [(pmdta)H][B(3,5-(CF_3)$_2$-C_6H_3)] (400 mg, 660 μmol) in THF dropwise at room temperature. After gas evolution ceased (approximately 15 min), the reaction mixture was filtered and the solvent volume was reduced in vacuo. Addition of *n*-pentane resulted in the precipitation of a colorless solid, which could be isolated by decantation and subsequently dried under reduced pressure. The product was obtained as a colorless solid (421 mg, 627 μmol, 95%). ^{1}H NMR (400 MHz, [D_8]THF): δ = 1.17 (t, ^3J(H,H) = 7.2 Hz, 12H; *N*-CH_2CH_3), 2.84–2.95 (m, 4H; *N*-CH_2CH_3), 2.96 (s, 4H; *N*-CH_2CH_2), 2.98–3.11 (m, 4H; *N*-CH_2CH_3), 3.73 (s, 4H; *para*-C_6H_3), 7.59 (s, 4H; *para*), 7.80 ppm (s, 8H; *ortho*-C_6H_3); ^{13}C{^{1}H} NMR (101 MHz, [D_8]THF): δ = 8.9 (*N*-CH_2CH_3), 47.0 (*N*-CH_2CH_3), 51.6 (*N*-CH_2CH_2), 118.3 (*para*-C_6H_3), 125.6 (q, ^1J(C,F) = 272.2 Hz, CF_3), 130.0 (qq, ^2J(C,F) = 31.52 Hz, ^3J(C,B) = 2.81 Hz, *meta*-C_6H_3), 135.7 (*ortho*-C_6H_3), 162.9 ppm (q, ^1J(B,C) = 49.9 Hz, *ipso*-C_6H_3). ^{11}B{^{1}H} NMR (128 MHz, [D_8]THF): δ = −6.50 ppm; ^{19}F{^{1}H} NMR (377 MHz, [D_8]THF): δ = −63.44 ppm; elemental analysis calcd (%) for $C_{41}H_{36}BF_{24}N_3Zn$: C 44.65, H 3.29, N 3.81; found: C 44.35, H 4.37, N 7.71.

Synthesis of 9a

Compound **8** (0.092 mmol, 0.100 g) was dissolved in THF (5 mL). The solution was pressurized with CO_2 (1.5 bar) and stirred for 5 min at room temperature. All volatile compounds were evaporated under vacuum (10^{-2} mbar) at room temperature, washed with *n*-pentane (2×5 mL), and dried to give **9** as a colorless powder. The compound was recrystallized from a mixture of THF and *n*-pentane at −30 °C (0.95 g, 96%). ^{1}H NMR (CD_3CN, 500 MHz): δ = 2.42 (s, 3H; NCH_3), 2.50 (s, 6H; NCH_3), 2.54 (s, 6H; NCH_3), 2.64 (m, 2H; NCH_2), 2.71 (m, 2H; NCH_2), 2.83 (m, 4H; NCH_2), 8.22 ppm (s, 1H; OC*H*O); ^{13}C{^{1}H} NMR (CD_3CN, 126 MHz): δ = 44.6 (NCH_3), 46.4 ({NCH_3}$_2$), 47.5 ({NCH_3}$_2$), 54.1 (NCH_2), 57.5 (NCH_2), 136.4 (*i*-C, C_6F_5), 138.3 (*p*-C, C_6F_5), 148.2 (*m*-C, C_6F_5), 150.1 (*o*-C, C_6F_5), 169.6 ppm (s, OCHO); ^{11}B NMR (CD_3CN, 128 MHz): δ = −16.66 ppm; ^{19}F NMR (CD_3CN, 471 MHz): δ = −133.76 (br s, *o*-C*F*), −163.94 (t, *p*-C*F*), −168.36 ppm (t, *m*-C*F*); elemental analysis calcd (%) for $C_{34}H_{24}BF_{20}N_3O_2Zn$: C 42.42, H 2.51, N 4.36; found: C 42.22, H 2.48, N 4.26;

Synthesis of 9b

A solution of **8b** (200 mg, 298 μmol) in THF was transferred to a Schlenk tube. The reaction mixture was degassed by three freeze–pump–thaw cycles and subsequently pressurized with CO_2 (1 bar). The solution was layered with *n*-pentane and stored at −30 °C. Overnight, colorless crystals formed, which were isolated by decantation and drying under high vacuum. The title complex was obtained as a colorless solid (208 mg, 292 μmol, 98%). ^{1}H NMR (400 MHz, [D_8]THF): δ = 2.10 (s, 24H; Ar-CH_3), 2.30 (s, 12H; *N*-CH_3), 2.17–2.52 (m, 11H; *N*-CH_2/*N*-CH_3), 6.38 (s, 4H; *para*-C_6H_3), 7.01 (s, 8H; *ortho*-C_6H_3), 8.21 ppm (s, 1H; Zn-OC*H*O); ^{13}C{^{1}H} NMR (101 MHz, [D_8]THF): δ = 21.3 (Ar-CH_3), 43.3 (*N*-CH_3), 45.4 (*N*-CH_3), 52.7 (*N*-CH_2), 56.2 (*N*-CH_2), 122.7 (*para*-C_6H_3), 132.1 (*meta*-C_6H_3), 134.5 (*ortho*-C_6H_3), 164.2 (q, ^1J(B,C) = 49.2 Hz, *ipso*-C_6H_3), 171.2 ppm (Zn-OCHO); ^{11}B{^{1}H} NMR (128 MHz, [D_8]THF): δ = −6.50 ppm; elemental analysis calcd (%) for $C_{84}H_{120}B_2N_6O_4Zn_2$: C 70.54, H 8.46, N 5.88; found: C 69.25, H 8.45, N 5.72.

Synthesis of 10a

Method A: [(pmdta)Zn(OCHO)]$_2$[B(3,5-Me_2-C_6H_3)$_4$]$_2$ (100 mg, 70 μmol) was dissolved in py (1 mL). The solution was layered with *n*-pentane and stored at −30 °C overnight. The title compound was obtained as a colorless solid (108 mg, 108 μmol, 98%).

Method B: A solution of **8b** (100 mg, 149 μmol) in py (1 mL) was degassed by three freeze–pump–thaw cycles and pressurized with CO_2 (1 bar). The solution was layered with *n*-pentane and stored at −30 °C overnight. The title compound was obtained as a colorless solid (113 mg, 143 μmol, 96%). ^{1}H NMR (400 MHz, [D_8]THF): δ =

© 2021 Wiley-VCH GmbH

2.10 (s, 24H; Ar-CH_3), 2.26 (s, 12H; *N*-CH_3), 2.28 (s, 3H; *N*-CH_3), 2.19–2.46 (m, 8H; *N*-CH_2), 6.38 (s, 4H; *para*-C_6H_3), 7.01 (s, 8H; *ortho*-C_6H_3), 7.18–7.39 (m, 2H; *meta*-C_6H_5N), 7.66 (t, ^3J(H,H) = 7.6 Hz, 1H; *meta*-C_6H_5N), 8.22 (s, 1H; Zn-OC*H*O), 8.53 ppm (dt, ^3J(H,H) = 4.4 Hz, ^4J(H,H) = 1.7 Hz, 2H; *ortho*-C_6H_5N); $^{13}C\{^1H\}$ NMR (101 MHz, [D$_8$]THF): δ = 19.4 (Ar-*C*H$_3$), 41.4 (*N*-*C*H$_3$), 43.5 (*N*-*C*H$_3$), 50.8 (*N*-*C*H$_2$), 54.4 (*N*-*C*H$_2$), 120.8 (*para*-C_6H_3), 121.6 (*meta*-C_5H_5N), 130.3 (*meta*-C_6H_3), 132.6 (*ortho*-C_6H_3), 133.6 (*para*-C_5H_5N), 147.9 (*ortho*-C_5H_5N), 162.9 (q, ^1J(B,C) = 49.2 Hz, *ipso*-C_6H_3), 169.2 ppm (Zn-OCHO); $^{11}B\{^1H\}$ NMR (128 MHz, [D$_8$]THF): δ = −6.95 ppm; elemental analysis calcd (%) for $C_{47}H_{65}BN_4O_2Zn$: C 71.08, H 8.25, N 7.05; found: C 69.76, H 7.88, N 7.48.

Synthesis of 10b

A solution of [(pmdta)ZnH][B(3,5-$(CF_3)_2C_6H_3)_4$] (100 mg, 90 μmol) in py (1 mL) was degassed by three freeze–pump–thaw cycles and pressurized with CO_2 (1 bar). The solution was layered with *n*-pentane and stored at −30 °C overnight. The title compound was obtained as a colorless solid (107 mg, 88 μmol, 97%). ^{1}H NMR (400 MHz, [D$_8$]THF): δ = 2.63 (d, J(H,H) = 36.1 Hz, 12H; *N*-CH_3), 2.66 (s, 3H; *N*-CH_3), 2.84–3.18 (m, 8H; *N*-CH_2), 7.40 (m, 2H; *meta*-C_5H_5N), 7.62 (s, 4H; *para*-C_6H_3), 7.79 (m, 1H; *para*-C_5H_5N), 7.84 (s, 8H; *ortho*-C_6H_3), 8.33 (s, 1H; Zn-OC*H*O), 8.61 ppm (m, 2H; *ortho*-C_5H_5N); $^{13}C\{^1H\}$ NMR (101 MHz, [D$_8$]THF): δ = 44.5 (*N*-*C*H$_3$), 46.7 (br, *N*-*C*H$_3$), 54.0 (*N*-*C*H$_2$), 57.7 (*N*-*C*H$_2$), 118.3 (*para*-C_6H_3), 125.0 (C_5H_5N-py), 125.6 (q, ^1J(C,F) = 272.2 Hz, *C*F$_3$), 130.1 (qq, ^2J(C,F) = 31.5 Hz, ^3J(C,B) = 2.8 Hz, *meta*-C_6H_3), 135.7 (*ortho*-C_6H_3), 137.6 (*para*-C_5H_5N), 150.7 (*ortho*- C_5H_5N), 162.9 (q, ^1J(B,C) = 49.9 Hz, *ipso*-C_6H_3), 173.0 ppm (Zn-O*C*HO); $^{11}B\{^1H\}$ NMR (128 MHz, [D$_8$]THF): δ = −6.50 ppm; $^{19}F\{^1H\}$ NMR (377 MHz, [D$_8$]THF): δ = −63.39 ppm; elemental analysis calcd (%) for $C_{47}H_{41}BF_{24}N_4O_2Zn$: C 46.04, H 3.37, N 4.57; found: C 44.13, H 3.84, N 4.76.

Hydrosilylation of CO_2 with $PhSiH_3$ by 8 and BPh_3

An NMR tube equipped with a J. Young valve was charged with compound **8** (0.004 g, 0.0043 mmol) and BPh_3 (0.001 g, 0.0043 mmol). [D$_3$]Acetonitrile (0.500 mL) was added to this mixture followed by $PhSiH_3$ (0.0535 mL, 0.434 mmol) and mesitylene (0.020 mL, 0.1446 mmol). The reaction mixture was degassed three times, and a constant pressure of CO_2 (1.5 bar) was maintained at 60 °C. The progress of the reaction was monitored by ^{1}H NMR spectroscopy for the consumption of $PhSiH_3$ (91% in 2 h). ^{1}H NMR (CD_3CN, 500 MHz): δ = 2.26 (s, 3H; Mes-CH_3), 6.81 (s, 1H; Mes-CH), 7.50 (t, ^3J(H,H) = 5 Hz, 1H; *p*-C_6H_5), 7.55 (t, ^3J(H,H) = 5 Hz, 2H; *m*-C_6H_5), 7.88 (d, ^3J(H,H) = 5 Hz, 2H; *o*-C_6H_5), 8.20 ppm (s, 3H; OC*H*O); $^{13}C\{^1H\}$ NMR (CD_3CN, 126 MHz): δ = 129.3 (*i*-C, C_6H_5), 129.4 (*p*-C, C_6H_5), 133.6 (*o*-C, C_6H_5), 135.4 (*m*-C, C_6H_5), 159.9 ppm (OCHO); chemical shift values corresponding to $PhSi(OCHO)_3$ are given.

Hydrosilylation of CO_2 with Ph_2SiH_2 by compound 8 and BPh_3

An NMR tube equipped with a J. Young valve was charged with compound **8** (0.008 g, 0.0081 mmol) and BPh_3 (0.002 g, 0.0081 mmol). [D$_3$]Acetonitrile (0.500 mL) was added to this mixture followed by $PhSiH_3$ (0.050 mL, 0.271 mmol) and mesitylene (0.037 mL, 0.271 mmol). The reaction mixture was degassed three times and a constant pressure of CO_2 (1.5 bar) was maintained at 60 °C for 8 h and at 75 °C for 10 h. The progress of the reaction was monitored by ^{1}H NMR spectroscopy for the consumption of Ph_2SiH_2 (98% in 24 h). ^{1}H NMR (CD_3CN, 500 MHz): δ = 2.25 (s, 3H; Mes-CH_3), 6.8 (s, 1H; Mes-CH), 7.50 (t, ^3J(H,H) = 5 Hz, 4H; *m*-C_6H_5), 7.59 (t, ^3J(H,H) = 5 Hz, 2H; *p*-C_6H_5), 7.77 (d, ^3J(H,H) = 5 Hz, 4H; *o*-C_6H_5), 8.26 ppm (s, 2H; OC*H*O); $^{13}C\{^1H\}$ NMR (CD_3CN, 126 MHz): δ = 129.2 (*i*-C, C_6H_5), 129.4 (*p*-C, C_6H_5), 133.0 (*o*-C, C_6H_5), 135.8 (*m*-C, C_6H_5), 160.4 ppm (OCHO)

Hydroboration of CO_2 with 1

An NMR tube equipped with a J. Young valve was charged with compound **1** (0.005 g, 0.0041 mmol). [D$_3$]Acetonitrile (0.500 mL) was added, followed by HBpin (0.0125 mL, 0.086 mmol) and mesitylene (0.004 mL, 0.028 mmol). The reaction mixture was degassed three times, and a constant pressure of CO_2 (1.5 bar) was maintained at 60 °C. The progress of the reaction was monitored by ^{1}H NMR spectroscopy for the consumption of HBpin (95% in 6 h). ^{1}H NMR (CD_3CN, 500 MHz): δ = 1.31 (s, 12H; CH_3), 2.26 (s, 3H; Mes-CH_3), 6.80 (s, 1H; Mes-CH), 8.41 ppm (s, 1H; OC*H*O); $^{13}C\{^1H\}$ NMR (CD_3CN, 126 MHz): δ = 24.9 (*C*H$_3$), 85.8 (*C*CH$_3$), 159.6 ppm (OCHO); ^{11}B NMR (CD_3CN, 128 MHz): δ = 22.63 ppm (OCHO*B*pin).

Hydroboration of CO_2 with 8

An NMR tube equipped with a J. Young valve was charged with compound **8** (0.008 g, 0.0081 mmol). [D$_3$]Acetonitrile (0.500 mL) was added, followed by HBpin (0.1175 mL, 0.81 mmol) and mesitylene (0.037 mL, 0.27 mmol). The reaction mixture was degassed three times, and a constant pressure of CO_2 (1.5 bar) was maintained at 60 °C. The progress of the reaction was monitored by ^{1}H NMR spectroscopy for the consumption of HBpin (94% in 2 h). ^{1}H NMR (CD_3CN, 500 MHz): δ = 1.31 (s, 12H; CH_3), 2.24 (s, 3H; Mes-CH_3), 6.80 (s, 1H; Mes-CH), 8.40 ppm (s, 1H; OC*H*O); $^{13}C\{^1H\}$ NMR (CD_3CN, 126 MHz): δ = 24.9 (*C*H$_3$), 85.8 (*C*CH$_3$), 159.6 ppm (OCHO); ^{11}B NMR (CD_3CN, 128 MHz): δ = 22.26 ppm (OCHOBpin).

Acknowledgements

We thank the IISER Thiruvananthapuram for generous funding and research facilities; the Alexander von Humboldt Foundation for a short-term (May–July, 2018) research fellowship for A.V. L.M. is a senior member of the Institut Universitaire de France and thanks CalMip for computational facilities.

Conflict of interest

The authors declare no conflict of interest.

Keywords: carbon dioxide reduction · hydroboration · hydrosilylation · reactive intermediates · zinc hydride

[1] R. B. King, *Encyclopedia of Inorganic Chemistry*, Wiley-VCH, Weinheim, **2006**.
[2] D. Seyferth, *Organometallics* **2001**, *20*, 2940–2955.
[3] S. Enthaler, *ACS Catal.* **2013**, *3*, 150–158.
[4] Y. Li, K. Junge, M. Beller, *Zinc Catal. Appl. Org. Synth.* **2015**, 5–32.
[5] R. J. Wehmschulte, L. Wojtas, *Inorg. Chem.* **2011**, *50*, 11300–11302.
[6] D. Specklin, F. Hild, C. Fliedel, C. Gourlaouen, L. F. Veiros, S. Dagorne, *Chem. Eur. J.* **2017**, *23*, 15908–15912.
[7] R. J. Procter, M. Uzelac, J. Cid, P. J. Rushworth, M. J. Ingleson, *ACS Catal.* **2019**, *9*, 5760–5771.
[8] A. Rit, T. P. Spaniol, J. Okuda, *Chem. Asian J.* **2014**, *9*, 612–619.
[9] P. Jochmann, D. W. Stephan, *Chem. Eur. J.* **2014**, *20*, 8370–8378.
[10] P. Jochmann, D. W. Stephan, *Angew. Chem. Int. Ed.* **2013**, *52*, 9831–9835; *Angew. Chem.* **2013**, *125*, 10014–10018.

 © 2021 Wiley-VCH GmbH

[11] J. L. Lortie, T. Dudding, B. M. Gabidullin, G. I. Nikonov, *ACS Catal.* **2017**, *7*, 8454 – 8459.
[12] W. Sattler, S. Ruccolo, M. Rostami Chaijan, T. Nasr Allah, G. Parkin, *Organometallics* **2015**, *34*, 4717 – 4731.
[13] C. Boone, I. Korobkov, G. I. Nikonov, *ACS Catal.* **2013**, *3*, 2336 – 2340.
[14] M. J. C. Dawkins, E. Middleton, C. E. Kefalidis, D. Dange, M. M. Juckel, L. Maron, C. Jones, *Chem. Commun.* **2016**, *52*, 10490 – 10492.
[15] Z. Mou, H. Xie, M. Wang, N. Liu, C. Yao, L. Li, J. Liu, S. Li, D. Cui, *Organometallics* **2015**, *34*, 3944 – 3949.
[16] R. K. Sahoo, M. Mahato, A. Jana, S. Nembenna, *J. Org. Chem.* **2020**, *85*, 11200 – 11210.
[17] P. A. Lummis, M. R. Momeni, M. W. Lui, R. McDonald, M. J. Ferguson, M. Miskolzie, A. Brown, E. Rivard, *Angew. Chem. Int. Ed.* **2014**, *53*, 9347 – 9351; *Angew. Chem.* **2014**, *126*, 9501 – 9505.
[18] I. D. Alshakova, G. I. Nikonov, *Synth.* **2019**, *51*, 3305 – 3312.
[19] A. K. Wiegand, A. Rit, J. Okuda, *Coord. Chem. Rev.* **2016**, *314*, 71 – 82.
[20] N. J. Brown, J. E. Harris, X. Yin, I. Silverwood, A. J. P. White, S. G. Kazarian, K. Hellgardt, M. S. P. Shaffer, C. K. Williams, *Organometallics* **2014**, *33*, 1112 – 1119.
[21] P. Jochmann, D. W. Stephan, *Organometallics* **2013**, *32*, 7503 – 7508.
[22] G. Ballmann, S. Grams, H. Elsen, S. Harder, *Organometallics* **2019**, *38*, 2824 – 2833.
[23] W. Sattler, G. Parkin, *J. Am. Chem. Soc.* **2011**, *133*, 9708 – 9711.
[24] D. M. Ermert, I. Ghiviriga, V. J. Catalano, J. Shearer, L. J. Murray, *Angew. Chem. Int. Ed.* **2015**, *54*, 7047 – 7050; *Angew. Chem.* **2015**, *127*, 7153 – 7156.
[25] M. Rauch, Y. Rong, W. Sattler, G. Parkin, *Polyhedron* **2016**, *103*, 135 – 140.
[26] S. Schulz, T. Eisenmann, D. Schuchmann, M. Bolte, M. Kirchner, R. Boese, J. Spielmann, S. Harder, *Zeitschr. Naturforsch. Sect. B.* **2009**, *64*, 1397 – 1400.
[27] A. Rit, T. P. Spaniol, L. Maron, J. Okuda, *Angew. Chem. Int. Ed.* **2013**, *52*, 4664 – 4667; *Angew. Chem.* **2013**, *125*, 4762 – 4765.
[28] R. Han, I. B. Gorrell, A. G. Looney, G. Parkin, *J. Chem. Soc. Chem. Commun.* **1991**, *10*, 717 – 719.
[29] K. Merz, M. Moreno, E. Löffler, L. Khodeir, A. Rittermeier, K. Fink, K. Kotsis, M. Muhler, M. Driess, *Chem. Commun.* **2008**, 73 – 75.
[30] M. Rombach, H. Brombacher, H. Vahrenkamp, *Eur. J. Inorg. Chem.* **2002**, 153 – 159.
[31] F. J. Fernández-Alvarez, L. A. Oro, *ChemCatChem* **2018**, *10*, 4783 – 4796.
[32] S. Dagorne, *Synth.* **2018**, *50*, 3662 – 3670.
[33] F. J. Fernández-Alvarez, A. M. Aitani, L. A. Oro, *Catal. Sci. Technol.* **2014**, *4*, 611 – 624.
[34] M. C. Lipke, A. L. Liberman-Martin, T. D. Tilley, *Angew. Chem. Int. Ed.* **2017**, *56*, 2260 – 2294; *Angew. Chem.* **2017**, *129*, 2298 – 2335.
[35] K. Kuciński, G. Hreczycho, *Green Chem.* **2020**, *22*, 5210 – 5224.
[36] M. L. Shegavi, S. K. Bose, *Catal. Sci. Technol.* **2019**, *9*, 3307 – 3336.
[37] W. Sattler, G. Parkin, *J. Am. Chem. Soc.* **2012**, *134*, 17462 – 17465.
[38] M. Rauch, G. Parkin, *J. Am. Chem. Soc.* **2017**, *139*, 18162 – 18165.
[39] A. Rit, A. Zanardi, T. P. Spaniol, L. Maron, J. Okuda, *Angew. Chem. Int. Ed.* **2014**, *53*, 13273 – 13277; *Angew. Chem.* **2014**, *126*, 13489 – 13493.
[40] G. Feng, C. Du, L. Xiang, I. Del Rosal, G. Li, X. Leng, E. Y. X. Chen, L. Maron, Y. Chen, *ACS Catal.* **2018**, *8*, 4710 – 4718.
[41] D. Specklin, C. Fliedel, C. Gourlaouen, J. C. Bruyere, T. Avilés, C. Boudon, L. Ruhlmann, S. Dagorne, *Chem. Eur. J.* **2017**, *23*, 5509 – 5519.
[42] J. C. Bruyere, D. Specklin, C. Gourlaouen, R. Lapenta, L. F. Veiros, A. Grassi, S. Milione, L. Ruhlmann, C. Boudon, S. Dagorne, *Chem. Eur. J.* **2019**, *25*, 8061 – 8069.
[43] F. Ritter, T. P. Spaniol, I. Douair, L. Maron, J. Okuda, *Angew. Chem. Int. Ed.* **2020**, *132*, 23535 – 23543.
[44] X. Wang, K. Chang, X. Xu, *Dalt. Trans.* **2020**, *49*, 7324 – 7327.
[45] Q. Zhang, N. Fukaya, T. Fujitani, J. C. Choi, *Bull. Chem. Soc. Jpn.* **2019**, *92*, 1945 – 1949.
[46] M. Tüchler, L. Gärtner, S. Fischer, A. D. Boese, F. Belaj, N. C. Mösch-Zanetti, *Angew. Chem. Int. Ed.* **2018**, *57*, 6906 – 6909.
[47] M. M. Deshmukh, S. Sakaki, *Inorg. Chem.* **2014**, *53*, 8485 – 8493.
[48] R. Chambenahalli, A. P. Andrews, F. Ritter, J. Okuda, A. Venugopal, *Chem. Commun.* **2019**, *55*, 2054 – 2057.
[49] D. Mukherjee, D. F. Sauer, A. Zanardi, J. Okuda, *Chem. Eur. J.* **2016**, *22*, 7730 – 7733.
[50] M. A. Beckett, G. C. Strickland, J. R. Holland, K. Sukumar Varma, *Polymer* **1996**, *37*, 4629 – 4631.
[51] U. Mayer, V. Gutmann, W. Gerger, *Monatsh. Chemie* **1975**, *106*, 1235 – 1257.
[52] M. A. D. D. F. Schriver, *The Manipulation of Air-Sensitive Compounds*, Wiley, **1986**.
[53] W. L. F. Armarego, C. L. L. Chai, *Purification of Laboratory Chemicals* **2013**, Elsevier.
[54] M. Ciampolini, N. Nardi, *Inorg. Chem.* **1966**, *5*, 41 – 44.
[55] M. Brookhart, B. Grant, A. F. Volpe, *Organometallics* **1992**, *11*, 3920 – 3922.
[56] R. Anulewicz-Ostrowska, T. Kliś, D. Krajewski, B. Lewandowski, J. Serwatowski, *Tetrahedron Lett.* **2003**, *44*, 7329 – 7331.
[57] A. J. Martínez-Martínez, A. S. Weller, *Dalton Trans.* **2019**, *48*, 3551 – 3554.

Manuscript received: December 17, 2020
Revised manuscript received: January 11, 2021
Accepted manuscript online: January 18, 2021
Version of record online: February 24, 2021

© 2021 Wiley-VCH GmbH